Nephrol Dial Transplant (2014) 29: 1514–1524
doi: 10.1093/ndt/gft336
Advance Access publication 22 October 2013

ndt
Nephrology Dialysis Transplantation

Original Article

Cardiac function and tolerance to ischemia–reperfusion injury in chronic kidney disease

James M. Kuczmarski[1,2], Christopher R. Martens[1], Shannon L. Lennon-Edwards[1,3] and David G. Edwards[1,2]

[1]Department of Kinesiology and Applied Physiology, University of Delaware, 25 N College Avenue, McDowell Hall, Newark, DE 19716, USA, [2]Department of Biological Sciences, University of Delaware, Newark, DE, USA and [3]Department of Behavioral Health and Nutrition, University of Delaware, Newark, DE, USA

Correspondence and offprint requests to: David G. Edwards; E-mail: dge@udel.edu, jmatthew@udel.edu

ABSTRACT

Background. Cardiac dysfunction is an independent risk factor of ischemic heart disease and mortality in chronic kidney disease (CKD) patients, yet the relationship between impaired cardiac function and tolerance to ischemia–reperfusion (IR) injury in experimental CKD remains unclear.

Methods. Cardiac function was assessed in 5/6 ablation–infarction (AI) and sham male Sprague–Dawley rats at 20 weeks of age, 8 weeks post-surgery using an isolated working heart system. This included measures taken during manipulation of preload and afterload to produce left ventricular (LV) function curves as well as during reperfusion following a 15-min ischemic bout. In addition, LV tissue was used for biochemical tissue analysis.

Results. Cardiac function was impaired in AI animals during preload and afterload manipulations. Cardiac functional impairments persisted post-ischemia in the AI animals, and 36% of AI animals did not recover sufficiently to achieve aortic overflow following ischemia (versus 0% of sham animals). However, for those animals able to withstand the ischemic perturbation, no difference was observed in percent recovery of post-ischemic cardiac function between groups. Urinary NOx (nitrite + nitrate) excretion was lower in AI animals and accompanied by reduced LV endothelial nitric oxide synthase and NOx. LV antioxidants superoxide dismutase-1 and -2 were reduced in AI animals, whereas glutathione peroxidase-1/2 as well as NADPH-oxidase-4 and H_2O_2 were increased in these animals.

Conclusions. Impaired cardiac function appears to predispose AI rats to poor outcomes following short-duration ischemic insult. These findings could be, in part, mediated by increased oxidative stress via nitric oxide-dependent and -independent mechanisms.

Keywords: cardiac dysfunction, cardiac ischemia–reperfusion injury, chronic kidney disease, nitric oxide, oxidative stress

INTRODUCTION

Chronic kidney disease (CKD) patients have an increased risk of developing and dying from ischemic heart disease (IHD) [1, 2]. IHD clinically presents, in part, as an increased rate of acute myocardial infarction (AMI) with a graded risk of mortality following AMI as renal disease progresses [3]. Although these ischemic cardiac events are predominately attributed to coronary artery disease, ~27% of all cases may also result from non-atherosclerotic disease [4]. Furthermore, symptomatic IHD is not a significant predictor of death independent of congestive heart failure [2]. Consequently, cardiac dysfunction and associated cardiomyopathy most likely play an important role in predisposing CKD patients to IHD and subsequent poor prognosis [1, 5].

Cardiac dysfunction with concomitant cardiomyopathy are evident early in advancing renal disease [6–8] and exist as independent risk factors of symptomatic IHD [2] and mortality [9, 10]. These epidemiological findings have been confirmed in studies conducted in uremic rats and *in vitro* cell culture experiments demonstrating impaired cardiac function [11, 12] in conjunction with left ventricular hypertrophy, abnormal cardiac energetics and altered calcium homeostasis [13, 14]. In contrast, the relationship between impaired cardiac function

and susceptibility to cardiac ischemia–reperfusion (IR) injury in experimental CKD remains unclear.

The primary pathological consequence of cardiac ischemic events is cardiac IR injury, in which significant reductions in coronary blood supply followed by restoration of blood flow elicit deleterious effects to the myocardium [15]. The purpose of the present investigation was to assess cardiac function and IR injury in the 5/6 ablation–infarction (AI) model of moderate-to-severe CKD. Cardiac function was measured in sham and AI male Sprague–Dawley rats using an *in vitro*-isolated working heart preparation [16]. This included measures taken during preload and afterload manipulation as well as pre-ischemia and between 15–30 min of reperfusion following a 15-min ischemic bout. This short period of ischemia has been shown to induce myocardial stunning, a form of cardiac IR injury characterized by reversible contractile dysfunction without resulting necrosis [15]. We hypothesized that baseline cardiac function would be impaired in CKD and associated with augmented myocardial stunning. In addition, the role of oxidative stress in kidney disease-related cardiac dysfunction and tolerance to IR injury was explored.

MATERIALS AND METHODS

Animals and experimental design

This experimental protocol was approved by the University of Delaware Animal Use and Care Committee and followed the guidelines established by the National Institutes of Health Office of Laboratory Animal Welfare for the use of animals in research.

Male Sprague–Dawley rats were housed in standard cages in a temperature/light-controlled environment and given free access to standard rat chow and water. Animals were randomly assigned to sham or AI study groups and, at 12 weeks of age, underwent surgery as previously described [17]. Briefly, all animals were anesthetized using isofluorane (1.0–5.0%) and shaved along their right and left lateral abdomen, just below the lowermost ribs, for access to each kidney. The AI animals then underwent 2/3 ligation of the renal artery branches supplying the left kidney and removal of the right kidney to induce CKD. Kidneys were exposed and manipulated in the sham animals with no ligation or ablation being performed. After surgery, animals were maintained over a period of 8 weeks to allow kidney disease progression until being sacrificed at 20 weeks of age. This period has been shown to elicit moderate-to-severe CKD in AI animals [17].

Renal function and urinary NOx (nitrite + nitrate) measurements

The animals were placed in metabolic cages 1 week prior to sacrifice with free access to water only, for an overnight (~16 h) urine collection. After the urine collection, volume of the urine was recorded and blood samples were collected from tail veins and centrifuged at 3000 r.p.m. for 10 min at 4°C for isolation of serum. The serum and urine samples were then stored at −80°C until further analysis.

Urine protein excretion was measured in urine samples using the Bradford method (sham: $n = 16$; AI: $n = 16$; replicates: $n = 3$) [18]. In addition, systemic nitric oxide (NO) production [19] was measured by assessing urinary excretion of the stable NO oxidation products, NO_2^- and NO_3^- (NO_2^- + NO_3^-: NOx), in the urine samples via the Greiss Reaction (sham: $n = 5$; AI: $n = 5$; replicates: $n = 3$; Cayman Chemical; Ann Arbor, MI). Serum samples were filtered with 10-kDa Amicon-Ultra centrifugal filters (EMD Millipore Corporation; Billerica, MA) and used to determine serum creatinine concentration with a colorimetric assay (sham: $n = 7$; AI: $n = 7$; replicates: $n = 3$; Cayman Chemical; Ann Arbor, MI).

Renal pathology

Glomerulosclerosis index (GSI) was used to assess kidney damage as previously described (sham: $n = 5$; AI: $n = 5$) [20, 21]. Left kidneys were dissected following sacrifice, and a transverse section was fixed in a 10% formalin solution. The samples were then sent to the University of Delaware Comparative Pathology Laboratory for periodic acid-Schiff staining (periodic acid-Schiff kit, #395B-1KT; Sigma-Aldrich; Saint Louis, MO) and GSI determination by an ACVP-certified anatomic pathologist blinded to the origin of each sample. Glomeruli (100 per sample) from 5-µm paraffin-embedded kidney sections were scored using a semi-quantitative scoring method to determine the degree of glomerular damage: grade 0, normal glomeruli; grade 1, sclerotic area ≤ 25% (minimal sclerosis); grade 2, sclerotic area 25–50% (moderate sclerosis); grade 3, sclerotic area 51–75% (moderate-to-severe sclerosis), and grade 4, sclerotic area ≥ 75% (severe sclerosis). GSI was determined as the total sum of scores divided by the number of glomeruli observed using the following formula: $GSI = (1 \times n_1) + (2 \times n_2) + (3 \times n_3) + (4 \times n_4)/n_0 + n_1 + n_2 + n_3 + n_4$, where n_x is the number of glomeruli in each grade of glomerulosclerosis [22].

Isolated perfused working heart

An isolated working heart preparation (Radnoti LLC; Monrovia, CA) was used to evaluate cardiac performance at baseline as well as pre- and post-ischemia as previously described [12, 23]. Animals were anesthetized using either an intraperitoneal injection of ketamine–xylazine (100 mg/kg) or inhalation of isofluorane (1.5–5.0%) for basal cardiac function and IR injury measurements, respectively. Hearts were rapidly excised and placed in an ice-cold saline solution until mass was measured on an electronic scale (gross wet mass). The aorta was then quickly cannulated and perfused in a retrograde fashion using a modified Krebs-Henseleit buffer (1.25 mM $CaCl_2$, 130 mM NaCl, 5.4 mM KCl, 11 mM glucose, 0.5 mM $MgCl_2$, 0.5 mM NaH_2PO_4, 25 mM $NaHCO_3$ and 12IU/l insulin; pH 7.4–7.5). The Krebs-Henseleit buffer was aerated with 95%O_2–5%CO_2, and the hearts were perfused at a constant temperature of ~37°C. After 15–20 min of retrograde perfusion, the hearts were switched to working heart mode and underwent experimental protocols for either baseline cardiac function or IR injury. Coronary and aortic flow rates were measured via timed collection of coronary effluent and aortic column overflow, respectively. Cardiac output (CO) was determined as the sum of coronary and aortic flow. Pressure

and heart rate (HR) measurements were taken from a luer fitting on the aortic cannula using a pressure transducer and instrument amplifier (Kent Scientific Corporation; Torrington, CT). Data were collected at 100 Hz using a BIOPAC-MP100 data acquisition system (Goleta, CA).

Baseline cardiac function. Basal cardiac function was assessed in a subset of animals by independently altering left atrial filling pressure (preload) and aortic pressure (afterload) to construct left ventricular function curves. Aortic pressure was initially held constant at 80-cm H_2O, and filling pressure was set at 9.5-, 13.5-, 17.5- and 21.5-cm H_2O in increments of 3–5 min to document the relationship between CO and preload (starling curve). Filling pressure was then held constant at 13.5-cm H_2O, and aortic pressure was set in increments of 3–5 min at 60-, 70-, 80-, 90- and 100-cm H_2O to establish the relationship between afterload and CO.

Cardiac IR injury. In a second subset of animals, cardiac function was measured pre- and post-short-duration cardiac ischemia. Pre-ischemic cardiac function was assessed at 13.5-cm H_2O of filling pressure with an 80-cm-high aortic column. Once cardiac function measures had stabilized, global and normothermic ischemia was initiated by turning off the working heart system perfusion pump and clamping atrial inflow and aortic outflow. The hearts remained in a water-jacketed chamber maintained at ~37°C during 15 min of ischemia. After ischemia, the hearts were perfused in a retrograde fashion for 15 min until being switched back to working heart mode for 15 min, for a total of 30 min of reperfusion. Post-ischemic cardiac function was recorded between 15 and 30 min of reperfusion in working heart mode.

Cardiac biochemical tissue measurements

An additional group of sham ($n = 8$) and AI ($n = 8$) animals were anesthetized using inhalation of isofluorane (1.5–5.0%), and the hearts were excised and mass measured similarly to those used for *in vitro* cardiac function. The hearts were then dissected for removal and sectioning of the left ventricle (LV). The LV sections were snap-frozen in liquid nitrogen and stored at −80°C until being used for cardiac biochemical measurements.

The LV tissue samples were homogenized using a Next-Advance BulletBlender®, according to the manufacturer's instructions (see Supplemental Methods). Cardiac NO substrate/production was assessed by measuring NOx (replicates: $n = 3$) and nitrotyrosine (replicates: $n = 3$) in LV tissue via the Greiss Reaction (Cayman Chemical; Ann Arbor, MI) and an OxiSelect™ Nitrotyrosine ELISA assay (Cell Biolabs, Inc; San Diego, CA), respectively. An Amplex® Red enzyme assay (Life Technologies; Carlsbad, CA) was used to measure LV hydrogen peroxide (H_2O_2; replicates: $n = 3$) in the presence and absence of catalase (1 KU/mL; Northwest Life Science Specialties; Vancouver, WA) to control for background fluorescence.

Western blotting. Protein abundance was detected in the LV tissue samples using western blotting (see Supplemental Methods).

Statistical analyses

For statistical comparison of animal characteristics and cardiac biochemical measurements between sham and AI animals, unpaired t-tests were used with Welch's corrections applied when appropriate. Two-way repeated-measures mixed model ANOVAs were used with Bonferonni post-hoc tests to compare cardiac function in baseline and IR experiments between groups at each pressure level and/or time-point. All statistical tests were performed using GraphPad Prism (GraphPad Software, Inc.; La Jolla, CA) with two-tailed probability values reported. Alpha was set at 0.05, and data are presented as mean values ± SEM.

RESULTS

Animal characteristics

Sham and AI group characteristics including average body mass, heart mass, renal function and renal pathology are summarized in Table 1. A considerable amount of muscle wasting has been reported in CKD [24], and here, body mass was lower in the AI animals ($P < 0.05$). Therefore, heart mass-to-tibia length was used as index of normalized heart mass and indicated significant cardiac hypertrophy in the AI animals. By design, AI was associated with significantly elevated protein excretion and serum creatinine confirming impaired renal function in these animals. Additionally, urine flow rate was increased in the AI animals ($P < 0.05$). This is thought to result, in part, from hyperfiltration and decreased fractional reabsorption in nephrons of the remnant kidney [25]. The AI animals also predominately displayed moderate-to-severe sclerotic kidney tissue and had significantly increased glomerulosclerosis as demonstrated by an elevated GSI score.

Table 1. Animal characteristics

	Sham	AI
Body mass and heart mass		
Body mass (g)	426 ± 9	373 ± 14*
Heart mass (g)	1.49 ± 0.06	1.70 ± 0.04*
Tibia length (cm)	4.3 ± 0.08	4.4 ± 0.07
Heart mass × tibia length^{-1} (mg/mm)	35 ± 1.3	39 ± 1.1*
Renal function		
Serum creatinine (mg/dl)	0.5 ± 0.06	2.5 ± 0.4*
Urine flow rate (ml × 24 h^{-1} × 100 g of body mass^{-1})	3.0 ± 0.4	8.2 ± 0.9*
Protein excretion (mg × 24 h^{-1} × 100 g of body mass^{-1})	5.8 ± 0.6	41.5 ± 4.9*
Renal pathology		
Glomerulosclerosis Index Score	0.16 ± 0.03	3.0 ± 0.17*
% Normal glomeruli (grade 0)	90.2 ± 2.8	2.9 ± 1.2*
% Minimal-to-moderate sclerosis (grades 1–2)	9.6 ± 2.8	28.6 ± 4.7*
% Moderate-to-severe sclerosis (grades 3–4)	0.2 ± 0.2	68.5 ± 5.8*

Characteristics of the Sham and AI animals including body mass and heart mass (sham $n = 16$, AI $n = 16$) as well as renal function (serum creatinine: sham $n = 7$, AI $n = 7$; urine flow rate and protein excretion: sham $n = 14$, AI $n = 14$) and pathology (sham $n = 5$, AI $n = 5$). Values are mean ± SEM. AI: 5/6 ablation–infarction rats;
*$P < 0.05$ versus sham.

Representative images of each grade of kidney sclerosis are shown in Figure 1 (see Supplemental Figure S1 for color image; available online).

Baseline cardiac function

AI animals presented with significantly impaired cardiac function and an inability to respond to different left atrial filling and aortic pressure perturbations (*see* Figure 2, Tables 2 and 3). CO was impaired in the AI animals at preloads of 13.5-, 17.5- and 21.5-cm H_2O (all $P < 0.05$), but not 9.5-cm H_2O ($P > 0.05$) while afterload was maintained at 80-cm H_2O (Figure 2A). CO was also impaired at afterloads of 60-, 70-, 80-, 90- and 100-cm H_2O with preload set at 13.5-cm H_2O ($P < 0.05$; Figure 2B). Tables 2 and 3 show CO and other measures of cardiac function taken during these experiments. Data points collected at 100-cm H_2O (Table 3) are not included due to the inability of some AI animals ($n = 3$) to achieve aortic overflow at this aortic pressure, and the AI animals unable to achieve aortic overflow during the entirety of afterload manipulations ($n = 1$) have been excluded. As shown, decreased CO was associated with systolic and diastolic dysfunction as indicated by decreased and altered rate of pressure development ($P < 0.05$). In addition, cardiac work and rate pressure product were decreased in the AI animals ($P < 0.05$), and no significant differences or changes in HR were observed throughout the baseline cardiac function experiments.

Cardiac IR injury

Approximately 36% of AI rat hearts failed to recover and achieve aortic overflow following 15 min of no-flow ischemia (4/11; versus 0% of sham animals, 0/8). Among those animals whose hearts recovered, CO and cardiac work were reduced relative to sham at baseline and following the ischemic insult ($P < 0.05$; Figure 3 and Table 4). In addition, AI animals demonstrated lower stroke volume and stroke work post-ischemia (SP × SV; $P < 0.05$ versus sham), whereas no significant differences were observed in HR or RPP (HR × SP) between groups (Table 4; Supplemental Figure S2). However, HR was reduced in the AI animals post-ischemia relative to baseline ($P < 0.05$). No significant differences in percent recovery of cardiac function among hearts that achieved post-ischemic aortic overflow were observed between the groups (Figure 3C and Table 4).

Biochemical measures of oxidative stress

Urinary NOx excretion was decreased in the AI animals ($P < 0.05$; Figure 4A) in conjunction with significantly decreased LV endothelial nitric oxide synthase (eNOS) expression

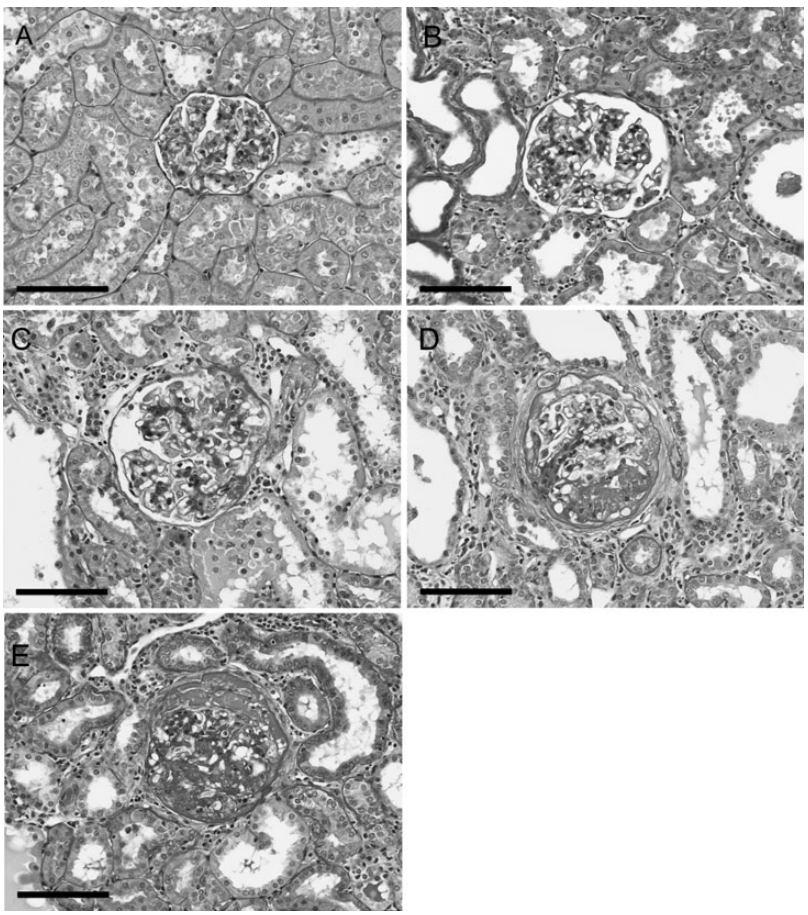

FIGURE 1: Representative images of periodic acid-Schiff-stained glomeruli with each grade of sclerosis including grade 0 (normal) (**A**), grade 1 (≤25% sclerotic area; minimal sclerosis) (**B**), grade 2 (25–50% sclerotic area; moderate sclerosis) (**C**), grade 3 (50–75% sclerotic area; moderate-to-severe sclerosis) (**D**) and grade 4 (≥75% sclerosis; severe sclerosis) (**E**). Images were taken at 200× magnification; ▬ 100 μm.

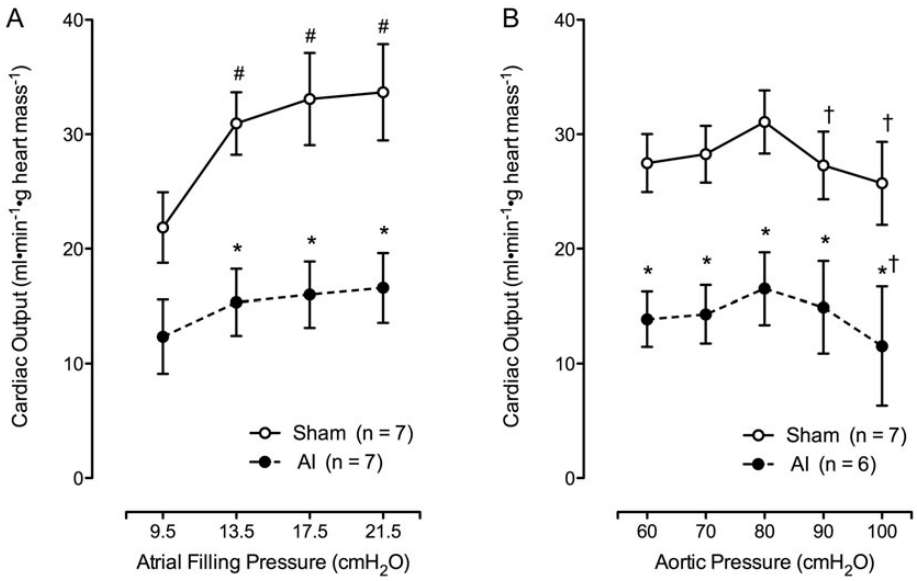

FIGURE 2: Left ventricular function curves depicting the relationship between CO and left ventricular filling pressure (**A**; sham: $n = 7$, AI: $n = 7$) as well as aortic pressure (**B**; sham: $n = 7$, AI: $n = 6$) in the sham and AI animals. The AI animals unable to achieve aortic overflow during the entirety of afterload manipulations ($n = 1$) have been excluded. As shown, CO was significantly impaired in the AI compared with the sham animals with increasing filling pressure and aortic pressure. Values are mean ± SEM; AI, 5/6 ablation–infarction animals, *$P < 0.05$ versus sham; #$P < 0.05$ versus 9.5 cm H_2O value; †$P < 0.05$ versus 80 cm H_2O value.

ORIGINAL ARTICLE

Table 2. Cardiac function during left atrial filling pressure manipulation

Left atrial filling pressure (cm H_2O)	9.5	13.5	17.5	21.5
Aortic pressure (cm H_2O)	80	80	80	80
Sham	280 ± 7	285 ± 8	287 ± 7	287 ± 7
AI	278 ± 16	285 ± 17	288 ± 18	286 ± 18
CO (mL × min^{-1} × g heart mass^{-1})				
Sham	22 ± 3	31 ± 3**	33 ± 4**	34 ± 4**
AI	12 ± 3	16 ± 3*	16 ± 3*	17 ± 3*
Coronary flow (mL × min^{-1} × g heart mass^{-1})				
Sham	10.2 ± 1.0	11.4 ± 0.9	12.0 ± 1.2	12.5 ± 1.5**
AI	6.0 ± 1.0	7.6 ± 1.2	7.7 ± 1.2	8.1 ± 1.6**
Systolic pressure (mmHg)				
Sham	83 ± 2	90 ± 2**	89 ± 2**	89 ± 2**
AI	71 ± 2*	74 ± 2*	74 ± 2*	74 ± 2*
Diastolic pressure (mmHg)				
Sham	41 ± 2	37 ± 2**	38 ± 1**	38 ± 2**
AI	45 ± 2	45 ± 2*	45 ± 1*	45 ± 1*
Cardiac work (SP × CO)				
Sham	1843 ± 294	2810 ± 291**	2981 ± 409**	3026 ± 417**
AI	915 ± 258	1151 ± 241*	1192 ± 226*	1246 ± 238*
RPP (HR × SP)				
Sham	23 181 ± 757	25 676 ± 841**	25 623 ± 844**	25 515 ± 944**
AI	19 856 ± 1398	20 902 ± 1154*	21 137 ± 1085*	21 112 ± 1092*
Maximum rate of ΔP (+dp/dt; mmHg × s^{-1})				
Sham	1238 ± 95	1437 ± 79**	1407 ± 77**	1415 ± 78**
AI	830 ± 104*	898 ± 61*	919 ± 43*	912 ± 63*
Minimum rate of ΔP (−dp/dt; mmHg × s^{-1})				
Sham	−894 ± 56	−1114 ± 47**	−1070 ± 50**	−1120 ± 72**
AI	−667 ± 73*	−669 ± 58*	−691 ± 46*	−710 ± 57*

Different measures of cardiac function in sham ($n = 7$) and 5/6 ablation–infarction (AI; $n = 7$) rats in response to altering atrial filling pressure.
Values are mean ± SEM; SP, systolic pressure; CO, cardiac output; RPP, rate pressure product; HR, heart rate; ΔP, change in pressure.
*$P < 0.05$ versus sham, **$P < 0.05$ versus 9.5-cm H_2O atrial filling pressure value.

Table 3. Cardiac function during aortic pressure manipulation

Left atrial filling pressure (cm H_2O)	13.5	13.5	13.5	13.5
Aortic pressure (cm H_2O)	60	70	80	90
HR (beats × min^{-1})				
Sham	279 ± 10	281 ± 11	287 ± 9	284 ± 10
AI	276 ± 23	282 ± 22	289 ± 19	278 ± 16
CO (mL × min^{-1} × g heart $mass^{-1}$)				
Sham	28 ± 3	28 ± 3	31 ± 3	27 ± 3**
AI	14 ± 2*	14 ± 3*	17 ± 3*	15 ± 4*
Coronary flow (mL × min^{-1} × g heart $mass^{-1}$)				
Sham	8.5 ± 0.9**	9.6 ± 1.0**	11.4 ± 1.0	11.5 ± 1.2
AI	5.9 ± 1.3**	6.7 ± 1.4	8.0 ± 1.3	7.5 ± 1.9
Systolic pressure (mmHg)				
Sham	76 ± 1**	82 ± 1**	90 ± 2	95 ± 2**
AI	59 ± 3*,**	64 ± 2*,**	74 ± 3*	80 ± 3*,**
Diastolic pressure (mmHg)				
Sham	29 ± 2**	33 ± 2**	37 ± 2	45 ± 2**
AI	35 ± 1**	40 ± 2**	45 ± 2*	52 ± 3**
Cardiac work (SP × CO)				
Sham	2086 ± 202**	2321 ± 227**	2813 ± 292	2321 ± 228
AI	842 ± 165*	935 ± 184*	1244 ± 263*	1254 ± 369*
RPP (HR × SP)				
Sham	21 095 ± 644**	22 964 ± 967**	25 743 ± 884	27 266 ± 1265**
AI	16 220 ± 1324*,**	17 972 ± 1299*,**	21 290 ± 1286*	22 296 ± 1667*
Maximum rate of ΔP (+dp/dt; mmHg × s^{-1})				
Sham	1312 ± 49	1415 ± 62	1442 ± 80	1431 ± 58
AI	827 ± 65*	825 ± 48*	923 ± 67*	919 ± 111*
Minimum rate of ΔP (−dp/dt; mmHg × s^{-1})				
Sham	−1052 ± 49	−1127 ± 93	−1103 ± 51	−1078 ± 48
AI	−607 ± 58*	−645 ± 56*	−687 ± 65*	−687 ± 99*

Different measures of cardiac function in sham ($n = 7$) and 5/6 ablation–infarction (AI; $n = 6$) rats in response to altering aortic pressure. Data collected at 100-cm H_2O are not included due to the inability of some AI animals ($n = 3$) to achieve aortic overflow, and AI animals unable to achieve aortic overflow during the entirety of afterload manipulations ($n = 1$) have been excluded.

Values are mean ± SEM; SP, systolic pressure; CO, cardiac output; RPP, rate pressure product; HR, heart rate; ΔP, change in pressure.

*P < 0.05 versus sham, **P < 0.05 versus 80-cm H_2O atrial filling pressure value.

(Figure 4C), NOx (Figure 4B), and nitrotyrosine (5.2 ± 0.76 versus 2.7 ± 0.32 nM mg of $protein^{-1}$, sham $n = 7$, AI $n = 7$). Similarly, two isoforms of the antioxidant enzyme, superoxide dismutase (SOD), were decreased in the AI rats (P < 0.05), whereas glutathione peroxidase (GPX-1/2) was increased (P < 0.05) and catalase was increased but not significantly in the AI animals (P = 0.24; Figure 5). No significant differences were observed in NADPH-oxidase isoform-2 (Nox-2) protein expression, but NADPH-oxidase isoform-4 (Nox-4) and H_2O_2 were increased in the LV of the AI rats (P < 0.05; Figure 6).

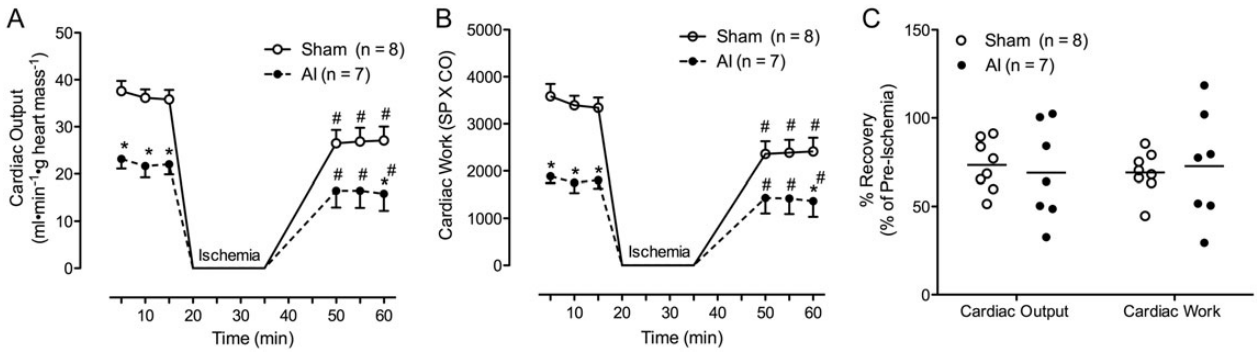

FIGURE 3: CO (**A**) and cardiac work (**B**) in the sham ($n = 8$) and AI ($n = 7$) animals able to withstand the 15-min ischemic bout (i.e. achieve aortic overflow post-ischemia) during the course of the ischemia–reperfusion perturbation at 5-, 10- and 15-min pre-ischemia as well as 20, 25 and 30 min post-ischemia. The CO and work were significantly impaired in the sham and AI animals post-ischemia relative to baseline. The AI animals also demonstrated impaired CO and work relative to the sham animals pre-ischemia and post-ischemia at 60 min. In contrast, no difference was observed in percent recovery (post-ischemic value/pre-ischemic value×100) of CO and work post-ischemia in the sham versus AI animals (**C**). Values are mean ± SEM (A and B) or mean with scatter plot distribution displayed (C); AI, 5/6 ablation–infarction animals, *P < 0.05 versus sham; #P < 0.05 versus 15-min pre-ischemia time-point.

ORIGINAL ARTICLE

Table 4. Cardiac function pre- and post-short-duration ischemia

	Sham ($n = 8$)			AI ($n = 7$)		
	Pre-I	Post-I	% Pre-I	Pre-I	Post-I	% Pre-I
HR (BPM)	277 ± 11	260 ± 13	94 ± 5	281 ± 14	238 ± 16**	85 ± 5
Coronary flow (mL × min^{-1} × g heart mass^{-1})	13.2 ± 0.9	12.7 ± 1.1	98 ± 7	7.9 ± 0.6*	6.9 ± 0.9*	86 ± 6
CO (mL × min^{-1} × g heart mass^{-1})	37 ± 2	27 ± 3**	73 ± 5	22 ± 2*	16 ± 4*,**	69 ± 10
Stroke volume (ul × beat^{-1} × g heart mass^{-1})	133 ± 9	104 ± 10**	78 ± 4	79 ± 5*	66 ± 11*	81 ± 10
Systolic pressure (mmHg)	94 ± 3	89 ± 4	95 ± 3	81 ± 3*	85 ± 3	104 ± 4
Diastolic pressure (mmHg)	36 ± 1	40 ± 2	110 ± 4	41 ± 1	41 ± 2	100 ± 5
Cardiac work (SP × CO)	3440 ± 226	2386 ± 279**	69 ± 4	1815 ± 171*	1407 ± 331*	73 ± 12
Stroke work (SP × SV)	12 608 ± 1077	9365 ± 1134**	74 ± 5	6449 ± 538*	5669 ± 1056*	86 ± 13
RPP (HR × SP)	25 948 ± 398	22 767 ± 548**	88 ± 2	22 745 ± 958*	20 075 ± 1510**	88 ± 5
Maximum rate of ΔP (+dp/dt; mmHg × s^{-1})	1663 ± 74	1487 ± 80	85 ± 4	1258 ± 57*	1201 ± 128	96 ± 10
Minimum rate of ΔP (−dp/dt; mmHg × s^{-1})	−1386 ± 65	−1169 ± 71**	90 ± 4	−1009 ± 39*	−1010 ± 68	101 ± 7

Different measures of cardiac function in sham ($n = 8$) and 5/6 ablation–infarction (AI; $n = 7$) rats pre- and post-15 min of ischemia in those animals able to withstand the ischemic perturbation (i.e. achieve post-ischemic aortic overflow).
Values are Mean ± SEM; SP, systolic pressure; CO, cardiac output; RPP, rate pressure product; HR, heart rate; ΔP, change in pressure.
*P < 0.05 versus sham, **P < 0.05 versus pre-ischemia.

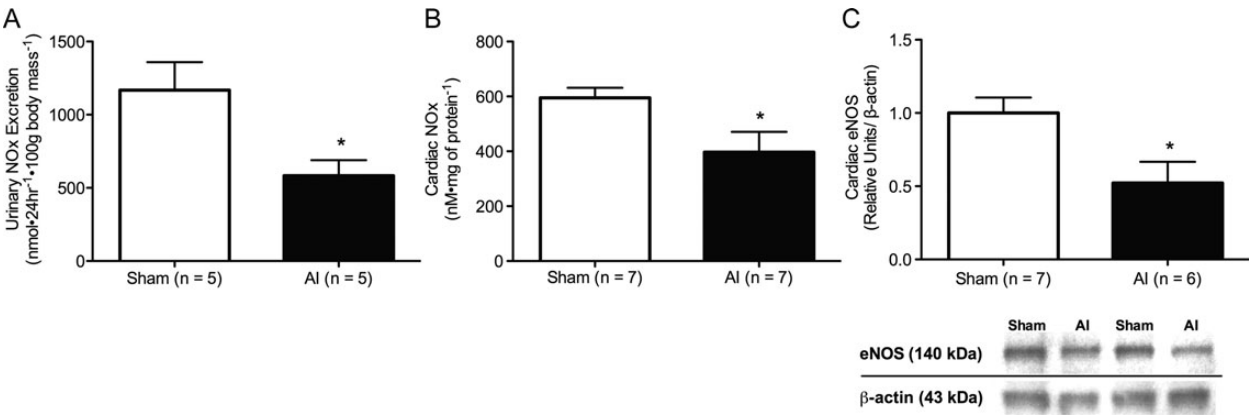

FIGURE 4: Urinary NOx (nitrite + nitrate) excretion (**A**; sham $n = 5$, AI $n = 5$), cardiac NOx (**B**; sham $n = 7$, AI $n = 7$), as well as a representative western blot and quantification of cardiac eNOS (**C**; sham $n = 7$, AI $n = 6$) in the sham and AI animals. Systemic nitric oxide and cardiac nitric oxide production were significantly reduced in the AI animals relative to the sham animals. Values are mean ± SEM; eNOS, endothelial nitric oxide synthase; AI, 5/6 ablation–infarction animals; *P < 0.05 versus sham.

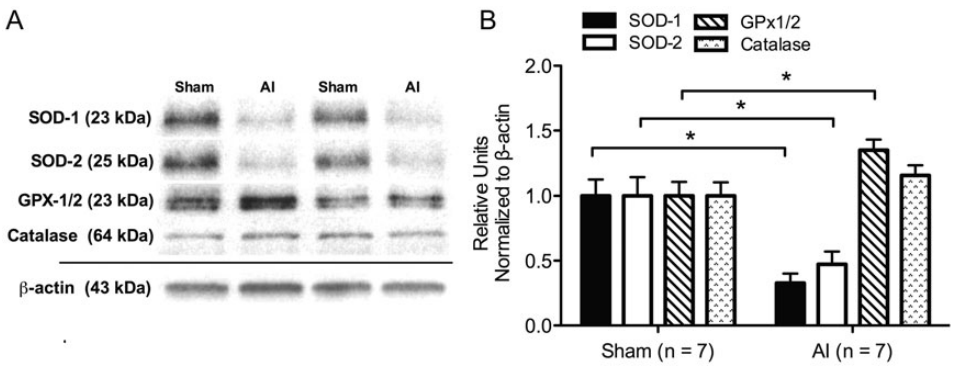

FIGURE 5: Representative western blots (**A**) and quantification (**B**) of cardiac antioxidant enzymes in the sham ($n = 7$) and AI ($n = 7$) animals. This includes superoxide dismutase-1 (SOD-1; MnSOD) and -2 (SOD-2; CuZnSOD), glutathione peroxidase 1/2 (GPx1/2) and catalase. SOD-1 and -2 were reduced in the AI animals compared with the sham animals, whereas GPx1/2 was significantly increased and catalase was increased but not significantly (P = 0.24) in the AI animals. Values are mean ± SEM; AI, 5/6 ablation–infarction animals; *P < 0.05 versus sham.

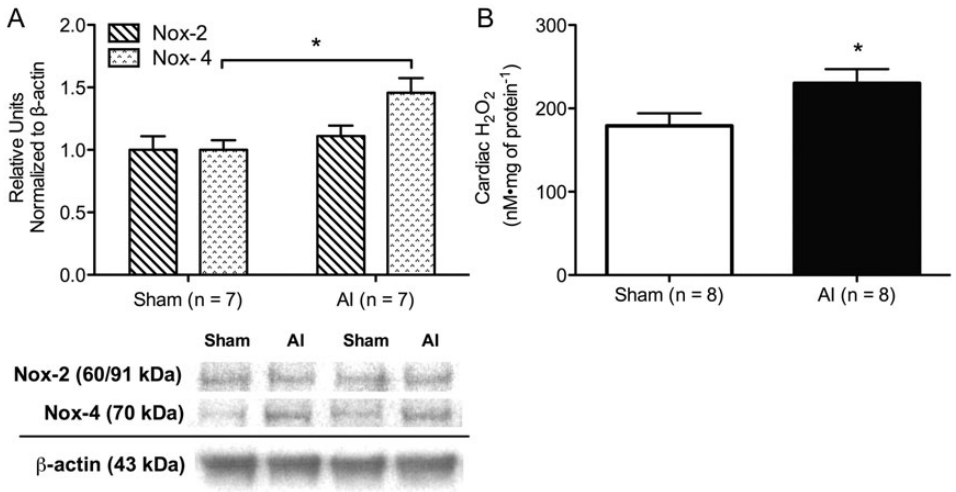

FIGURE 6: Representative western blots and quantification of cardiac NADPH-oxidase isoform-2 (Nox-2) and -4 (Nox-4) (**A**; sham: $n = 7$, AI: $n = 7$) as well as H_2O_2 production (**B**; sham: $n = 8$, AI: $n = 8$) in the sham and AI animals. Nox-4 and H_2O_2 were significantly increased in the AI animals compared with the sham animals, but no difference was observed in Nox-2 expression between groups. Values are mean ± SEM; AI, 5/6 ablation–infarction animals; *P < 0.05 versus sham.

DISCUSSION

To our knowledge, this is the first investigation to examine cardiac function and tolerance to short-duration cardiac IR injury (i.e. myocardial stunning) in the AI model of moderate-to-severe CKD. The AI animals presented with impaired baseline cardiac performance and heterogeneous responses to 15 min of global no-flow ischemia. For those AI animals able to withstand this ischemic perturbation, no differences in percent recovery of CO and cardiac work were observed compared with the sham controls. However, ∼36% of the isolated AI hearts did not recover enough to achieve aortic overflow, and absolute measures of cardiac function indicated persistent functional impairments with IR insult. These findings suggest that myocardial stunning is not augmented in AI, but impaired cardiac function may result in poor outcomes following short-duration ischemia.

Previous studies of cardiac function in experimental CKD have reported conflicting results. Subtotal 5/6 nephrectomy (NX) has been shown to induce cardiac dysfunction 4 and 10 weeks post-surgery in male and female Wistar rats, respectively [11, 12], whereas cardiac function remained unchanged compared with controls 8 weeks following NX elsewhere (Sprague–Dawley rats) [26]. In addition, the relationship between baseline cardiac performance and IR injury following short-duration ischemia has not been well characterized. To date, one study has been conducted to assess cardiac function pre- and post-ischemia following a 20-min ischemic bout in NX using an isolated working heart preparation [11]. Surprisingly, the investigators concluded that despite diminished cardiac function at baseline, tolerance to ischemia was enhanced in female Wistar NX rats as indicated by improved percent recovery of contractile function.

In the present investigation, we demonstrate cardiac dysfunction 8 weeks following AI that persists after 15 min of global no flow ischemia during reperfusion in male Sprague–Dawley rats. Post-ischemic cardiac dysfunction in the AI animals may be the result of both inotropic and chronotropic effects. Stroke volume and stroke work were reduced in the AI animals post-ischemia in conjunction with lower HR relative to baseline. Nevertheless, post-ischemic aortic overflow was not achieved in a subset of AI animals, and no differences were observed in percent recovery of those animals able to withstand ischemia compared with the controls. Discrepancies in results between our study and previous investigation could be attributed to the variation in the experimental design as well as the animal models used. Specifically, studies of cardiac function conducted thus far [11, 12, 26] have used the NX model of moderate CKD characterized by slowly progressing kidney damage and mild hypertension [27, 28]. In contrast, the AI model has been described as an accelerated hypertensive model of CKD with significant glomerulosclerosis and reduced systemic NO production [27, 29–31]. In the present study, moderate-to-severe glomerulosclerosis, decreased urinary NOx excretion and significant cardiac hypertrophy were demonstrated in the AI group. This more advanced uremic phenotype could be responsible for the significant reductions in cardiac function and poor outcomes with IR insult observed. Further, our ischemic perturbation was performed in the absence of potential sex-related cardioprotective effects including estrogen-induced protection during cardiac IR injury [32].

Among the factors contributing to the pathogenesis of cardiac disease in AI, oxidative stress most likely plays an essential role in this process. Oxidative stress is classically defined as an imbalance between reactive oxygen species (ROS) production and removal by endogenous antioxidants [33]. ROS include superoxide (O_2^-) and H_2O_2 that are produced via NADPH-oxidases (Noxs) and uncoupling of the electron transport chain at complex I in the failing heart [34, 35]. ROS can have various harmful effects on the myocardium

if produced in excess without adequate sequestration by antioxidant enzymes [36]. This includes disruption of ionic homeostasis, damage to the cell membrane and mitochondrial injury implicated in cardiac dysfunction and IR insult [15, 37, 38]. Additionally, ROS diminish the bioavailability of NO, which has been shown to be cardioprotective [39, 40] and essential for normal cardiac function in humans [41] and various animal models [42–45].

Oxidative stress is increased in AI animals and may be important in the development and progression of kidney disease in these rats [29]. Moreover, ROS have been shown to contribute to hypertension [46] and cardiac hypertrophy [47] in experimental CKD, and Noxs as well as ROS are increased in the LV of NX [47, 48] suggesting a pro-oxidant state in the uremic heart. Here, we explored potential pathways by which oxidative stress may influence cardiac dysfunction and IR intolerance in AI via NO-dependent and -independent mechanisms.

The AI animals demonstrated increased expression of cardiac Nox-4 but not Nox-2. Nox-4 is predominantly localized in the mitochondria of cardiac myocytes and is a major source of O_2^- and/or H_2O_2 in the failing heart [38], whereas Nox-2 represents a membrane-associated multisubunit protein complex that is analogous to phagocytic Nox and produces O_2^- [33]. Differential expression of Nox isoforms could indicate the source of uremic cardiac pathology, as Nox-4 is primarily involved in pressure overload–induced cardiomyopathy [38, 49].

In conjunction with increases in Nox-4, AI animals demonstrated increased expression of cardiac H_2O_2. H_2O_2 is readily produced enzymatically from O_2^- via dismutation by the antioxidant enzyme SOD. It is then either converted to $H_2O + O_2$ via the antioxidant enzymes, glutathione peroxidase and catalase, or the highly reactive hydroxyl radical ($^{\cdot}OH$) by the Fenton reaction [34, 37]. LV SOD-1 and SOD-2 were reduced in AI, whereas glutathione peroxidase and catalase were increased in these animals. This suggests several different related mechanisms of oxidative signaling in the AI heart: (i) O_2^- may not be effectively sequestered given the deficiency of SOD; (ii) H_2O_2 has been shown to degrade SOD through $^{\cdot}OH$ production [50] and may be feeding back on its own enzymatic production; (iii) H_2O_2 production from other sources other than SOD may be increased and (iv) GPx and catalase are increased in response to elevated H_2O_2 levels. Among the other possible sources of H_2O_2, cardiac Nox-4 represents a probable candidate [51, 52]; however, the stable form of H_2O_2, urea hydrogen peroxide, has also been shown to be increased in uremia [53].

Taken together, these findings suggest a pro-oxidant state in the AI heart with increased ROS production and altered antioxidant defense. Although we did not demonstrate augmented myocardial stunning in AI, cardiac dysfunction was evident at baseline and persisted post-ischemia with 36% of the AI hearts not recovering. Therefore, increased cardiac oxidative stress has implications in uremic cardiac dysfunction and ischemic intolerance, but short-duration oxidative IR injury may not be accentuated in AI. Regardless, oxidative stress could be contributing to impaired cardiac function pre- and post-ischemia indirectly through inhibition of NO as well as directly through ROS-induced oxidative injury. ROS, such as O_2^-, have been shown to inhibit NO production by oxidation of critical cofactors essential for NO synthesis, increasing endogenous NOS inhibitors, and reacting with NO to form the damaging reactive nitrogen species, $ONOO^-$ [54–56]. This could have obvious detrimental effects at the heart considering that inhibition of enzymatic production of NO is associated with systolic dysfunction in humans [41] and animal models [42–44], including uremia [45]. Furthermore, NO is thought to be protective against cardiac IR injury by reducing calcium sensitivity via protein s-nitrosylation [39] and the secondary messenger cyclic-GMP [40]. Consistent with previous reports [57], our data show that NO is decreased systemically and in the heart in CKD, a finding that could be partially mediated by increased oxidative stress. This includes reductions in cardiac eNOS and stored NO-metabolites (NOx). Conversely, $ONOO^-$ was not increased in AI as indicated by reduced nitrotyrosine levels. Nevertheless, nitrotyrosine formation is dependent upon NO production and could further reflect the decreased NO synthesis shown in these animals.

Potential direct effects of oxidative-induced cardiac injury in CKD include those mediated by Nox-4 and downstream O_2^- and/or H_2O_2. Nox-4, potentially via O_2^- and/or H_2O_2, has been linked to mitochondrial and subsequent LV dysfunction in heart failure [38]. Further, O_2^- and H_2O_2 are implicated in cardiac dysfunction associated with IR injury [15, 37]. Specifically, H_2O_2 has been proposed to contribute to cardiac contractile dysfunction at baseline and during IR insult by disrupting calcium homeostasis either directly through ATP depletion or indirectly via activation of the Na^+/H^+ exchanger [37]. Interestingly, activation of the Na^+/H^+ exchanger by H_2O_2 is thought to induce Na+ influx and subsequent calcium overload via the Na^+/Ca^{2+}-exchanger [37], which has increased expression and activity levels in experimental CKD [13, 14].

CONCLUSION

Decreased cardiac performance appears to predispose AI rats to poor outcomes following a short-duration ischemic insult. This impaired cardiac function and ischemic intolerance in AI could be, in part, mediated by increased levels of ROS and altered antioxidant defense via NO-dependent and -independent mechanisms. Additional study is needed to further delineate the role of oxidative stress in cardiac dysfunction and IR injury in CKD. This would include investigation involving pharmacological as well as non-pharmacological interventions to improve cardiac antioxidant status and NO production.

SUPPLEMENTARY DATA

Supplementary data are available online at http://ndt.oxfordjournals.org.

ACKNOWLEDGEMENTS

The authors thank Dr. Erin Brannick and Joanne Kramer of the University of Delaware CANR Comparative Pathology Laboratory for their assistance in determining glomerulosclerosis index. The authors also acknowledge Taylor Schellhardt and Jahyun Kim for their assistance with data collection. This work was supported by National Institutes of Health (NIH) grants P20 RR016472-12 and P20 GM103446-12.

CONFLICT OF INTEREST STATEMENT

None declared.

REFERENCES

1. Parfrey PS, Foley RN. Ischemic heart disease in chronic uremia. Blood purificat 1996; 14: 321–326
2. Parfrey PS, Foley RN, Harnett JD *et al.* Outcome and risk factors of ischemic heart disease in chronic uremia. Kidney int 1996; 49: 1428–1434
3. U S Renal Data System, USRDS 2012. Annual Data Report: Atlas of Chronic Kidney Disease and End-Stage Renal Disease in the United States. Bethesda, MD: National Institutes of Health, National Institute of Diabetes and Digestive and Kidney Diseases, 2012
4. Rostand SG, Kirk KA, Rutsky EA. Dialysis-associated ischemic heart disease: insights from coronary angiography. Kidney int 1984; 25: 653–659
5. Curtis BM, Parfrey PS. Congestive heart failure in chronic kidney disease: disease-specific mechanisms of systolic and diastolic heart failure and management. Cardiology clin 2005; 23: 275–284
6. Pehrsson SK, Jonasson R, Lins LE. Cardiac-performance in various stages of renal-failure. Brit Heart J 1984; 52: 667–673
7. Nardi E, Palermo A, Mulè G *et al.* Left ventricular hypertrophy and geometry in hypertensive patients with chronic kidney disease. J Hypertens 2009; 27: 633–641
8. Levin A, Thompson CR, Ethier J *et al.* Left ventricular mass index increase in early renal disease: impact of decline in hemoglobin. Am J Kidney Dis 1999; 34: 125–134
9. Cerasola G, Nardi E, Palermo A *et al.* Epidemiology and pathophysiology of left ventricular abnormalities in chronic kidney disease: a review. J Nephrol 2011; 24: 1–10
10. Parfrey PS, Foley RN, Harnett JD *et al.* Outcome and risk factors for left ventricular disorders in chronic uraemia. Nephrol Dial Transpl 1996; 11: 1277–1285
11. Tutterova M, Vavrinkova H, Bohdanecka M *et al.* Effect of chronic renal insufficiency on the function and metabolic parameters of the isolated rat heart. Physiol Res 1997; 46: 427–433
12. Raine AE, Symour AM, Roberts AF *et al.* Impairment of cardiac function and energetics in experimental renal failure. J Clin Invest 1993; 92: 2934–2940
13. McMahon AC, Naqvi RU, Hurst MJ *et al.* Diastolic dysfunction and abnormality of the Na+/Ca2+ exchanger in single uremic cardiac myocytes. Kidney Int 2006; 69: 846–851
14. Kennedy D, Omran E, Periyasamy SM *et al.* Effect of chronic renal failure on cardiac contractile function, calcium cycling, and gene expression of proteins important for calcium homeostasis in the rat. J Am Soc Nephrol 2003; 14: 90–97
15. Powers SK, Murlasits Z, Wu M *et al.* Ischemia-reperfusion-induced cardiac injury: a brief review. Med Sci Sport Exer 2007; 39: 1529–1536
16. Sutherland FJ, Hearse DJ. The isolated blood and perfusion fluid perfused heart. Pharmacol Res 2000; 41: 613–627
17. Chen GF, Baylis C. In vivo renal arginine release is impaired throughout development of chronic kidney disease. Am j physiol 2010; 298: F95–F102
18. Bradford MM. A rapid and sensitive method for the quantitation of microgram quantities of protein utilizing the principle of protein-dye binding. Anal Biochem 1976; 72: 248–254
19. Baylis C, Vallance P. Measurement of nitrite and nitrate levels in plasma and urine - what does this measure tell us about the activity of the endogenous nitric oxide system? Curr Opin Nephrol Hy 1998; 7: 59–62
20. Moningka NC, Sindler AL, Muller-Delp JM *et al.* Twelve weeks of treadmill exercise does not alter age-dependent chronic kidney disease in the Fisher 344 male rat. J Physiol 2011; 589(Pt 24): 6129–6138
21. Raij L, Azar S, Keane W. Mesangial immune injury, hypertension, and progressive glomerular damage in Dahl rats. Kidney Int 1984; 26: 137–143
22. Maric C, Sandberg K, Hinojosa-Laborde C. Glomerulosclerosis and tubulointerstitial fibrosis are attenuated with 17Œ≤-estradiol in the aging dahl salt sensitive Rat. J Am Soc Nephrol 2004; 15: 1546–1556
23. Lennon SL, Quindry J, Hamilton KL *et al.* Loss of exercise-induced cardioprotection after cessation of exercise. J Appl Physiol 2004; 96: 1299–1305
24. Workeneh BT, Mitch WE. Review of muscle wasting associated with chronic kidney disease. Am J Clin Nutr 2010; 91: 1128S–1132S
25. Kwon TH, Frokiaer J, Knepper MA *et al.* Reduced AQP1, -2, and -3 levels in kidneys of rats with CRF induced by surgical reduction in renal mass. Am J Physiol 1998; 275(5 Pt 2): F724–F741
26. Hatori N, Havu N, Hofman-Bang C *et al.* Myocardial morphology and cardiac function in rats with renal failure. Jpn Circ J 2000; 64: 606–610
27. Griffin KA, Picken M, Bidani AK. Method of renal mass reduction is a critical modulator of subsequent hypertension and glomerular injury. J Am Soc Nephrol 1994; 4: 2023–2031
28. Griffin KA, Picken MM, Churchill M *et al.* Functional and structural correlates of glomerulosclerosis after renal mass reduction in the rat. J Am Soc Nephrol 2000; 11: 497–506
29. Sasser JM, Moningka NC, Tsarova T *et al.* Nebivolol does not protect against 5/6 ablation/infarction induced chronic kidney disease in rats - comparison with angiotensin II receptor blockade. Life Sci 2012; 91: 54–63
30. Szabo AJ, Wagner L, Erdely A *et al.* Renal neuronal nitric oxide synthase protein expression as a marker of renal injury. Kidney Int 2003; 64: 1765–1771
31. Erdely A, Wagner L, Muller V *et al.* Protection of wistar furth rats from chronic renal disease is associated with maintained renal nitric oxide synthase. J Am Soc Nephrol 2003; 14: 2526–2533
32. Deschamps AM, Murphy E, Sun J. Estrogen receptor activation and cardioprotection in ischemia reperfusion injury. Trends Cardiovas Med 2010; 20: 73–78
33. Cave AC, Brewer AC, Narayanapanicker A *et al.* NADPH oxidases in cardiovascular health and disease. Antioxid Redox Sign 2006; 8: 691–728
34. Finkel T, Holbrook NJ. Oxidants, oxidative stress and the biology of ageing. Nature 2000; 408: 239–247
35. Ide T, Tsutsui H, Kinugawa S *et al.* Mitochondrial electron transport complex I is a potential source of oxygen free radicals in the failing myocardium. Circ Res 1999; 85: 357–363
36. Dhalla AK, Singal PK. Antioxidant changes in hypertrophied and failing guinea pig hearts. Am J Physiol 1994; 266: H1280–H1285
37. Taylor RP, Ciccolo JT, Starnes JW. Effect of exercise training on the ability of the rat heart to tolerate hydrogen peroxide. Cardiovas Res 2003; 58: 575–581
38. Kuroda J, Ago T, Matsushima S *et al.* NADPH oxidase 4 (Nox4) is a major source of oxidative stress in the failing heart. P Natl Acad Sci US A 2010; 107: 15565–15570
39. Sun J, Murphy E. Protein S-nitrosylation and cardioprotection. Circ Res 2010; 106: 285–296
40. Francis SH. The role of cGMP-dependent protein kinase in controlling cardiomyocyte cGMP. Circ Res 2010; 107: 1164–1166
41. Stamler JS, Loh E, Roddy MA *et al.* Nitric oxide regulates basal systemic and pulmonary vascular resistance in healthy humans. Circulation 1994; 89: 2035–2040
42. Gardiner SM, Compton AM, Kemp PA *et al.* Regional and cardiac haemodynamic effects of NG-nitro-L-arginine methyl ester in conscious, Long Evans rats. Br J Pharmacol 1990; 101: 625–631

43. Klabunde RE, Ritger RC, Helgren MC. Cardiovascular actions of inhibitors of endothelium-derived relaxing factor (nitric oxide) formation/release in anesthetized dogs. Eur J Pharm 1991; 199: 51–59
44. Moreno H, Jr., Metze K, Bento AC *et al.* Chronic nitric oxide inhibition as a model of hypertensive heart muscle disease. Basic Res Cardiol 1996; 91: 248–255
45. Bongartz LG, Braam B, Verhaar MC *et al.* Transient nitric oxide reduction induces permanent cardiac systolic dysfunction and worsens kidney damage in rats with chronic kidney disease. Am J Physiol2010; 298: R815–RR23
46. Hasdan G, Benchetrit S, Rashid G *et al.* Endothelial dysfunction and hypertension in 5/6 nephrectomized rats are mediated by vascular superoxide. Kidney Int 2002; 61: 586–590
47. Michea L, Villagran A, Urzua A *et al.* Mineralocorticoid receptor antagonism attenuates cardiac hypertrophy and prevents oxidative stress in uremic rats. Hypertension 2008; 52: 295–300
48. Bai Y, Sigala W, Adams GR *et al.* Effect of exercise on cardiac tissue oxidative and inflammatory mediators in chronic kidney disease. Am J Nephrol 2009; 29: 213–221
49. Byrne JA, Grieve DJ, Bendall JK *et al.* Contrasting roles of NADPH oxidase isoforms in pressure-overload versus angiotensin II-induced cardiac hypertrophy. Circ Res 2003; 93: 802–805
50. Choi SY, Kwon HY, Kwon OB *et al.* Hydrogen peroxide-mediated Cu,Zn-superoxide dismutase fragmentation: protection by carnosine, homocarnosine and anserine. Biochi Biophys Acta 1999; 1472: 651–657
51. Serrander L, Cartier L, Bedard K *et al.* NOX4 activity is determined by mRNA levels and reveals a unique pattern of ROS generation. Biochem J 2007; 406: 105–114
52. Takac I, Schr√∂der K, Zhang L *et al.* The E-loop is involved in Hydrogen Peroxide Formation by the NADPH oxidase Nox4. J Biol Chem 2011; 286: 13304–13313
53. Moh A, Sakata N, Takebayashi S *et al.* Increased production of urea hydrogen peroxide from Maillard reaction and a UHP-Fenton pathway related to glycoxidation damage in chronic renal failure. J Am Soc Nephrol 2004; 15: 1077–1085
54. Baylis C. Nitric oxide deficiency in chronic kidney disease. Am J Physiol 2008; 294: F1–F9
55. Guzik TJ, Harrison DG. Vascular NADPH oxidases as drug targets for novel antioxidant strategies. Drug Discov Today 2006; 11: 524–533
56. Martens CR, Edwards DG. Peripheral vascular dysfunction in chronic kidney disease. Cardiol Res Pract 2011; 2011: 267257
57. Vaziri ND, Ni Z, Oveisi F *et al.* Enhanced nitric oxide inactivation and protein nitration by reactive oxygen species in renal insufficiency. Hypertension 2002; 39: 135–141

Received for publication: 7.2.2013; Accepted in revised form: 29.6.2013